Experimental measurement of charged kaon semileptonic decay branching fraction $K^- \to e^- \bar{\nu}_e \pi^0$ using ISTRA+ detector

V.A. Uvarov, S.A. Akimenko, G.I. Britvich, A.P. Filin, A.V. Inyakin, S.A. Kholodenko, A.S. Konstantinov, V.F. Konstantinov, V.M. Leontiev, V.F. Obraztsov, V.A. Polyakov, A.V. Popov, V.I. Romanovsky, O.V. Stenyakin, O.G. Tchikilev, O.P. Yushchenko

Institute for High Energy Physics, Protvino, Russia

V.N. Bolotov, V.A. Duk, A.A. Khudyakov, A.I. Makarov, A.Yu. Polyarush

Institute for Nuclear Research, Moscow, Russia

Abstract

The ratio of decay rates for $K^- \to e^- \bar{\nu}_e \pi^0$ and $K^- \to \pi^- \pi^0$ decays has been measured using the ISTRA+ spectrometer. The result of our measurement is the following:

$$\mathcal{R}_{K_{e3}/K_{2\pi}} = 0.2423 \pm 0.0015\,(stat) \pm 0.0037\,(syst). \quad (1)$$

Using the current PDG value for the $K^- \to \pi^- \pi^0$ branching fraction, this result leads to the measured branching fraction of $Br(K_{e3}) = 0.0501 \pm 0.0009$ and to the value of $|V_{us}|\, f_+(0) = 0.2115 \pm 0.0021$.

1 Introduction

The charged kaon semileptonic decay channel $K^- \to e^- \bar{\nu}_e \pi^0$ (K_{e3}) is one of interesting channels in investigating the V_{us} element in the Cabibbo–Kobayashi–Maskawa (CKM) three-generation quark mixing matrix. This element is determined from the individual semileptonic decay width $\Gamma(K^- \to e^- \bar{\nu}_e \pi^0)$ extracted from the measured ratio

$$\mathcal{R}_{K_{e3}/K_{2\pi}} \equiv \frac{\Gamma(K_{e3})}{\Gamma(K_{2\pi})} \equiv \frac{\Gamma(K^- \to e^- \bar{\nu}_e \pi^0)}{\Gamma(K^- \to \pi^- \pi^0)} \tag{2}$$

and from the PDG average decay rate of the $K^- \to \pi^- \pi^0$ normalisation mode. The decay rate $\Gamma(K_{e3})$ can be written as follows [1]:

$$\Gamma(K_{e3}) = \frac{G_{\rm F}^2 \, m_K^5}{384\pi^3} \, S_{EW} \, |V_{us}|^2 \, |f_+(0)|^2 \, (1 + \delta_K^e) \, I_K^e, \tag{3}$$

where $G_{\rm F}$ is the Fermi constant, m_K is the kaon mass, S_{EW} is the short-distance radiative correction, $f_+(0)$ is the calculated form factor at zero momentum transfer ($t = 0$) for the $e^- \bar{\nu}_e$ system, and the term

$$(1 + \delta_K^e) \simeq (1 + \delta_{SU(2)}^e + \delta_{EM}^e)^2 \tag{4}$$

is the model-dependent long-distance correction with contributions due to isospin breaking in strong (SU(2)) and electromagnetic (EM) interactions [2]. Theory is needed for S_{EW}, $f_+(0)$, $\delta_{SU(2)}^e$ and δ_{EM}^e. The term I_K^e is the result of the phase space integration after factoring out $f_+(0)$, and is defined as [1]:

$$\begin{aligned} I_K^e = \frac{1}{m_K^8} \int_{m_e^2}^{(m_K - m_\pi)^2} \frac{{\rm d}t}{2t^3} \, (t - m_e^2)^2 \, T^{1/2}(t, m_K^2, m_\pi^2) \\ \times \{ T(t, m_K^2, m_\pi^2) \, (2t + m_e^2) \, |f_+(t)/f_+(0)|^2 \\ + 3 m_e^2 \, (m_K^2 - m_\pi^2)^2 \, |f_0(t)/f_+(0)|^2 \}, \end{aligned} \tag{5}$$

where $T(x,y,z) \equiv x^2+y^2+z^2-2xy-2xz-2yz$; m_π and m_e are the masses of the π^0 and the e^-, respectively; $f_+(t)$ and $f_0(t)$ are the vector and the scalar form factors corresponding to the angular momentum configuration of the $K-\pi$ system. The form factors $f_+(t)$ and $f_0(t)$ can be described using the following approximations:

$$f_+(t) \;=\; f_+(0)\left(1+\lambda'_+\,\frac{t}{m^2_{\pi^\pm}}+\frac{1}{2}\,\lambda''_+\,\frac{t^2}{m^4_{\pi^\pm}}\right) \tag{6}$$

and

$$f_0(t) \;=\; f_+(0)\left(1+\lambda_0\,\frac{t}{m^2_{\pi^\pm}}\right), \tag{7}$$

where $f_+(0)$ is obtained from theory, and λ'_+, λ''_+ and λ_0 are measured [3, 4].

Our previous measurement of the ratio (2) can be found in Ref. [5]. In the present study the new measurement of this ratio is presented. The contribution from internal bremsstrahlung is included for the $K^- \to e^-\bar{\nu}_e\pi^0$ decay mode. This paper is organized as follows. The experimental setup is described in Sect. 2. The event selection and all corrections applied to the data are presented in Sect. 3. The analysis and sources of the systematic uncertainty are described in Sect. 4. The result and its comparision with theory and its impact on V_{us} are given in Sect. 5.

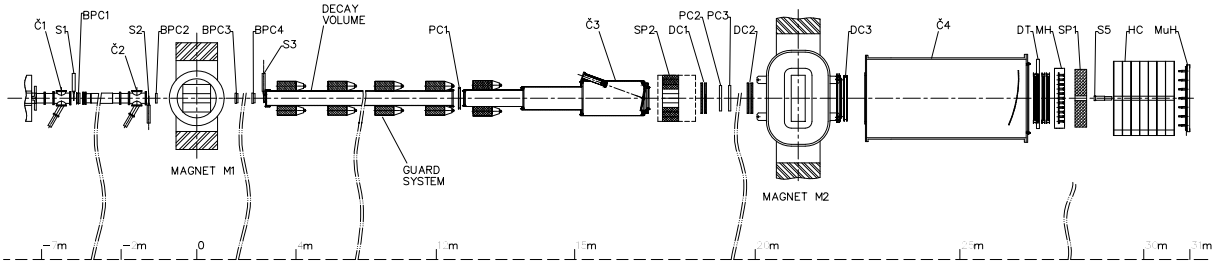

Figure 1: The side elevation view of the ISTRA+ detector.

2 Experimental setup

The experiment has been performed at the IHEP proton synchrotron U-70 with the experimental apparatus ISTRA+, which is a modification of the ISTRA-M setup [6] and which was described in some details in our papers where studies of the K^-_{e3} [7], $K^-_{\mu 3}$ [8] and $K^-_{\pi 3}$ [9] decays were presented. The setup is located in the negative unseparated secondary beam with the following parameters during the measurement: the momentum is ~ 25 GeV/c with $\sigma(p)/p \sim 1.5\,\%$, the admixture of kaons is $\sim 3\,\%$, and the total intensity is $\sim 3{\times}10^6$ per spill.

The side elevation view of the ISTRA+ detector is shown in Fig. 1. The setup coordinate system is the following: the x, y and z axes are turned along the field of the spectrometer magnet M2, the vertical line and the setup longitudinal axis, respectively.

The measurement of the beam particles, deflected by the beam magnet M1, is performed with four beam proportional chambers BPC1–BPC4. The kaon identification is done by three threshold gas Cherenkov counters Č0–Č2 (Č0 is not shown in Fig. 1). The momenta of the secondary charged particles, deflected in the vertical plane by the spectrometer magnet M2, are measured with three proportional chambers PC1–PC3, three drift chambers DC1–DC3 and four planes of the drift tubes DT. The secondary photons are detected by the lead-glass electromagnetic calorimeters SP1 and SP2. To veto low

energy photons the decay volume is surrounded by the guard system of eight lead-glass rings and by the SP2. The wide aperture threshold helium Cherenkov counters Č3 and Č4 are not used in the present study. In Fig. 1, HC is a scintillator-iron sampling hadron calorimeter, MH is a scintillation hodoscope used to improve the time resolution of the tracking system, MuH is a scintillation muon hodoscope.

The trigger is provided by the scintillation counters S1–S5, the Cherenkov counters Č0–Č2 and the analog sum of the amplitudes from the last dinodes of the calorimeter SP1 (see Refs. [7, 8] for details). The latter serves to suppress the dominating $K^- \to \mu^- \bar{\nu}_\mu$ decay.

3 Event selection

About 332 M events were collected during one physics run in Winter 2001. These experimental data are complemented by about 260 M events generated with the Monte Carlo program GEANT3 [10]. The Monte Carlo simulation includes a realistic description of the experimental setup: the decay volume entrance windows, the track chamber windows, gas mixtures, sense wires and cathode structures, the Cherenkov counter mirrors and gas mixtures, the showers development in the electromagnetic calorimeters, etc. The details of the reconstruction procedure have been published in Refs. [7, 8], here only key points relevant to the $K^- \to e^- \bar{\nu}_e \pi^0$ and $K^- \to \pi^- \pi^0$ events selection are described.

The data processing starts with the beam track reconstruction in the beam proportional chambers BPC1–BPC4, and then with the secondary tracks reconstruction in the decay tracking system PC1–PC3, DC1–DC3 and DT. The decay vertex is reconstructed by means of the unconstrained vertex fit of the beam and decay tracks. Finally, the electromagnetic showers are looked for in the calorimeters SP1 and SP2, and the photons are reconstructed using the fit procedure with the Monte Carlo generated two-dimensional patterns of showers. To suppress hadronic contamination in the $K^- \to e^- \bar{\nu}_e \pi^0$ events and leptonic contamination in the $K^- \to \pi^- \pi^0$ events the particle identification is used. The electrons are identified using the ratio of the energy of the shower, detected in the calorimeter SP1 and associated with the track of the electron, to the momentum of the electron [7]. The muons are identified using the information from the calorimeters SP1 and HC [8].

In the present study, the main purpose of the event selection is to suppress significantly all components of the background contamination. The expediency of the selection criteria, mentioned below, is motivated by the Monte Carlo investigation.

At *the first step* of the event selection only the measurements of the beam and secondary charged particles are used. Those events are selected which satisfy the following requirements (the corresponding passing ratios $\mathcal{P}$ are given in parenthesis):

- only one beam track and one negative secondary track are detected;
- the decay vertex is before the chamber PC1, 5 m $< z <$ 11 m, and its transverse position is in the region of -3 cm $< x <$ 3 cm and -2 cm $< y <$ 6 cm ($\mathcal{P} = 0.23$);
- the probability of the vertex fit is in the region of $0.1 < CL(\chi^2) < 0.9$ ($\mathcal{P} = 0.53$);
- the angle between the K^- line of flight and the direction in the K^- rest frame of the secondary track, taken with π^- mass, is in the region of $-0.8 < \cos\theta^*_{\pi^-} < 0.8$ ($\mathcal{P} = 0.89$);
- the first hit of the secondary track is either in the chamber PC1, or in the DC1, or in the PC2, while the last hit of this track is in the drift tubes DT ($\mathcal{P} = 0.91$).

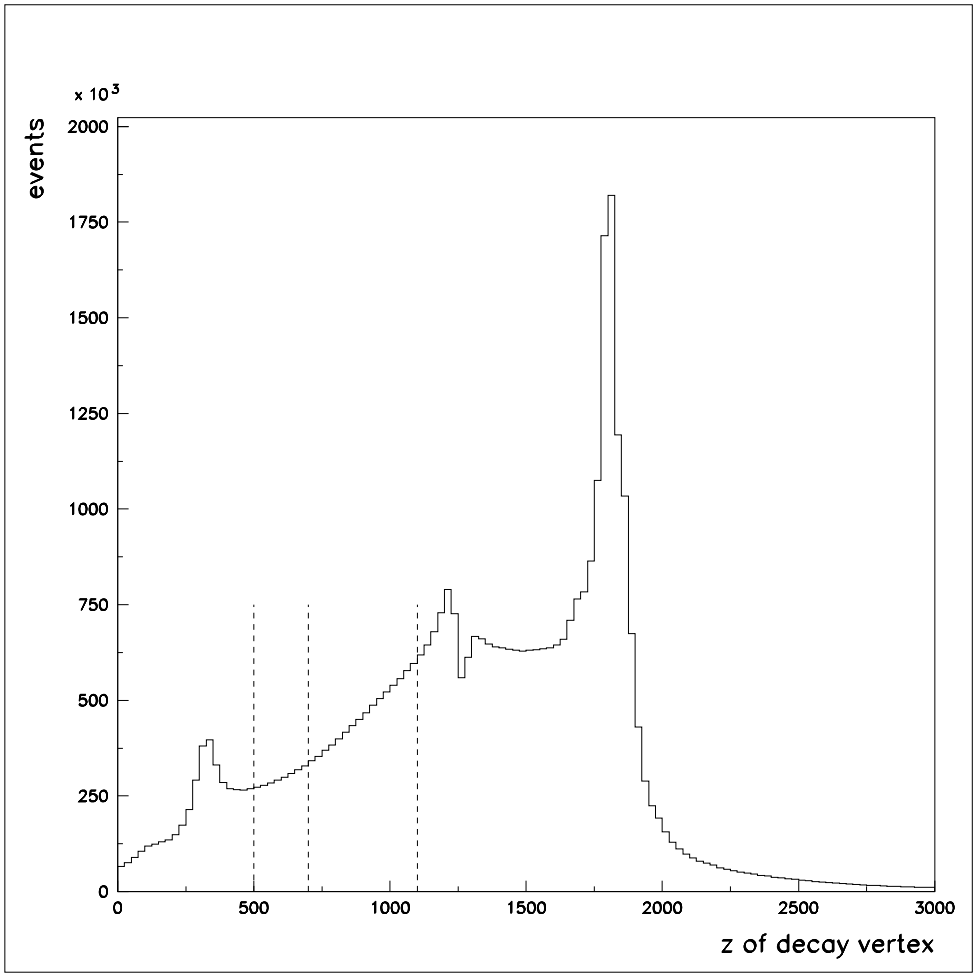
x 10^3
events
2000
1750
1500
1250
1000
750
500
250
0
0
500
1000
1500
2000
2500
3000
z of decay vertex

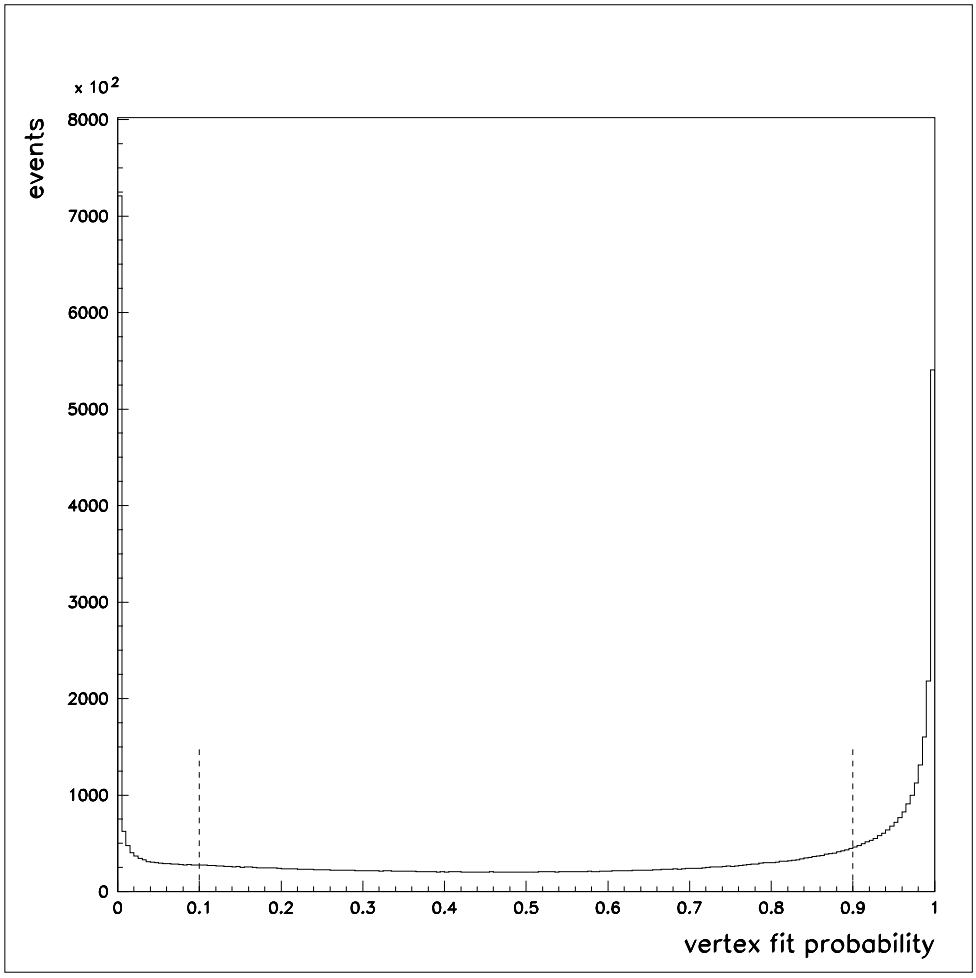
x 10^2
events
8000
7000
6000
5000
4000
3000
2000
1000
0
0
0.1
0.2
0.3
0.4
0.5
0.6
0.7
0.8
0.9
1
vertex fit probability

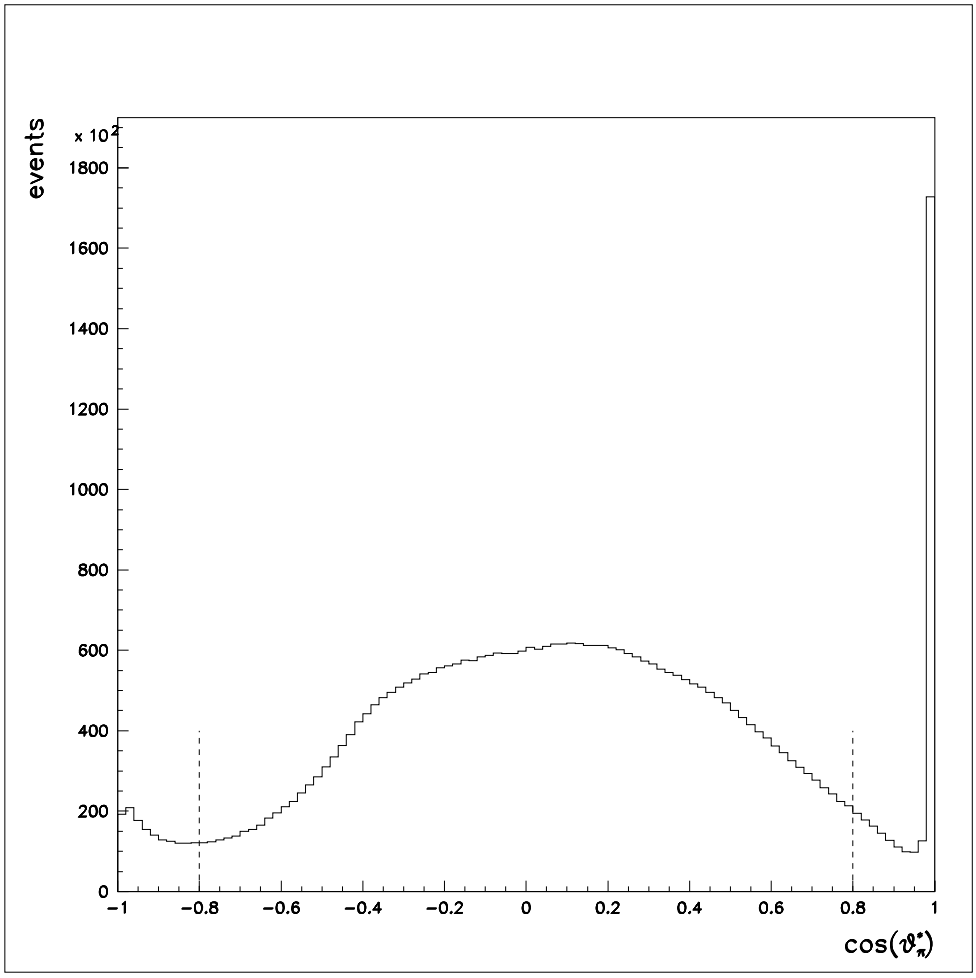
events
x 10²
1800
1600
1400
1200
1000
800
600
400
200
0
−1
−0.8
−0.6
−0.4
−0.2
0
0.2
0.4
0.6
0.8
1
cos(ϑ*π)

At *the second step* of the event selection the measurements of the showers in the calorimeters SP1 and SP2 are used. Associating the SP1 shower with the secondary track is done if the distance $R = [(x_{sh} - x_{tr})^2 + (y_{sh} - y_{tr})^2]^{1/2}$ is less than 3 cm, where (x_{sh}, y_{sh}) and (x_{tr}, y_{tr}) are the transverse coordinates of the shower and of the track extrapolation to the calorimeter SP1, respectively. The showers, which are not associated with the secondary track, are considered as the photons. The $\gamma\gamma$ pair with the smallest value of the deviation $|M(\gamma\gamma) - m_{\pi^0}|$, where $M(\gamma\gamma)$ is the effective mass of the $\gamma\gamma$ pair and m_{π^0} is the π^0 mass, is considered as the $\pi^0 \to \gamma\gamma$ decay product. Other photons are considered as the prompt photons. The event selection at this step is done by the requirements:

- the total number of photons in both calorimeters is equal to two or three;
- the energy of each photon is more than 1 GeV;
- the photon configuration is not such as the one, in which all photons are reconstructed from one and the same cluster of overlapped showers ($\mathcal{P} = 0.99$);
- the distance $R = [(x_{sh} - x_{tr})^2 + (y_{sh} - y_{tr})^2]^{1/2}$ of each SP1 photon is more than 15 cm ($\mathcal{P} = 0.94$);
- the value of the deviation $|M(\gamma\gamma) - m_{\pi^0}|$, calculated for the $\gamma\gamma$ pair taken as the π^0 decay product, is less than 0.03 GeV ($\mathcal{P} = 0.90$);
- in case when the prompt photon is detected, the angle between this photon and the secondary track direction is less than 10 mrad ($\mathcal{P} = 0.98$).

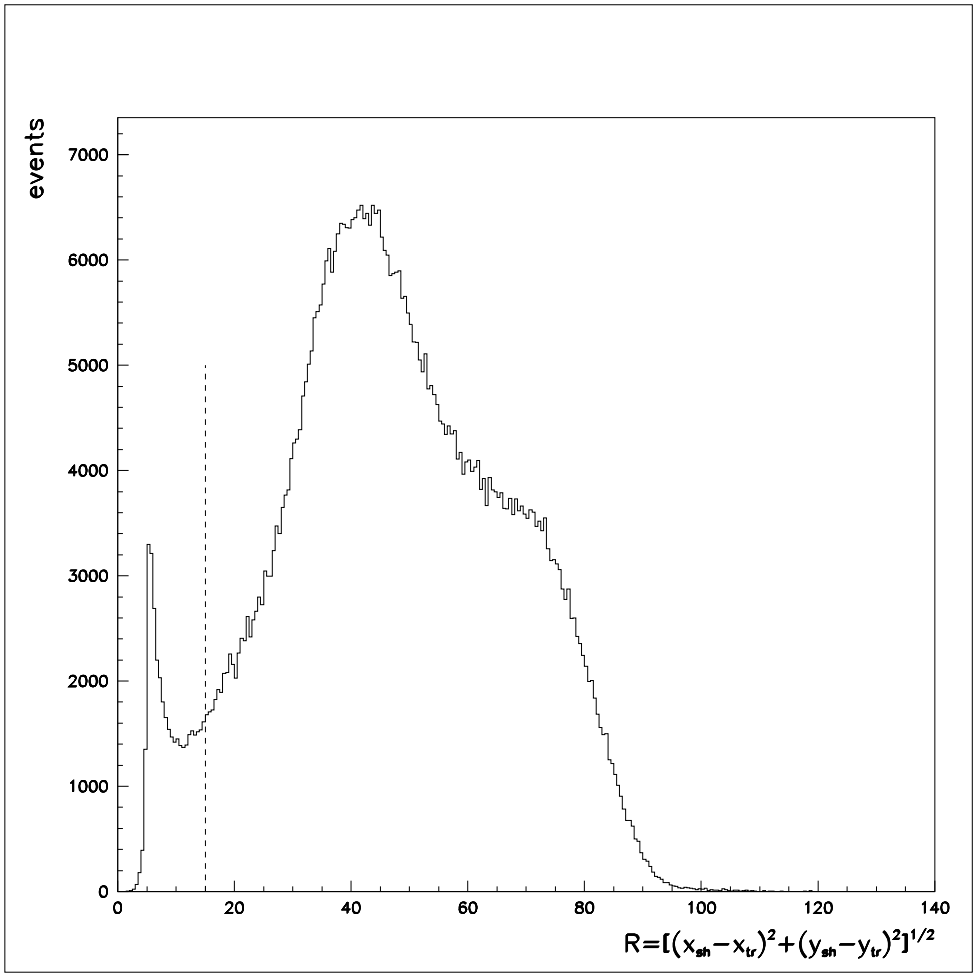
events
7000
6000
5000
4000
3000
2000
1000
0
0
20
40
60
80
100
120
140
R=[(x_sh−x_tr)^2+(y_sh−y_tr)^2]^1/2

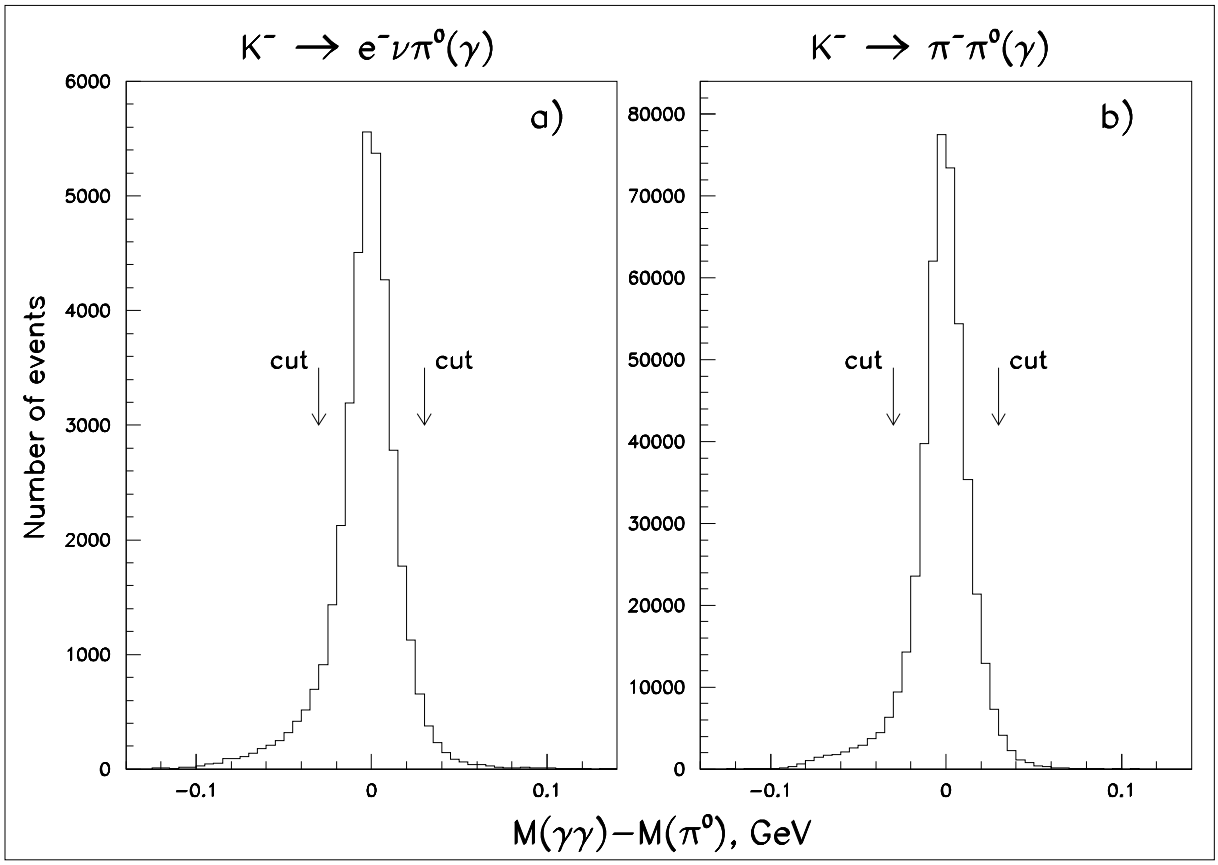

Figure 2: The deviations of the $\gamma\gamma$ effective masses from the π^0 mass in the $K^- \to e^-\bar{\nu}_e\pi^0$ events (**a**) and in the $K^- \to \pi^-\pi^0$ events (**b**).

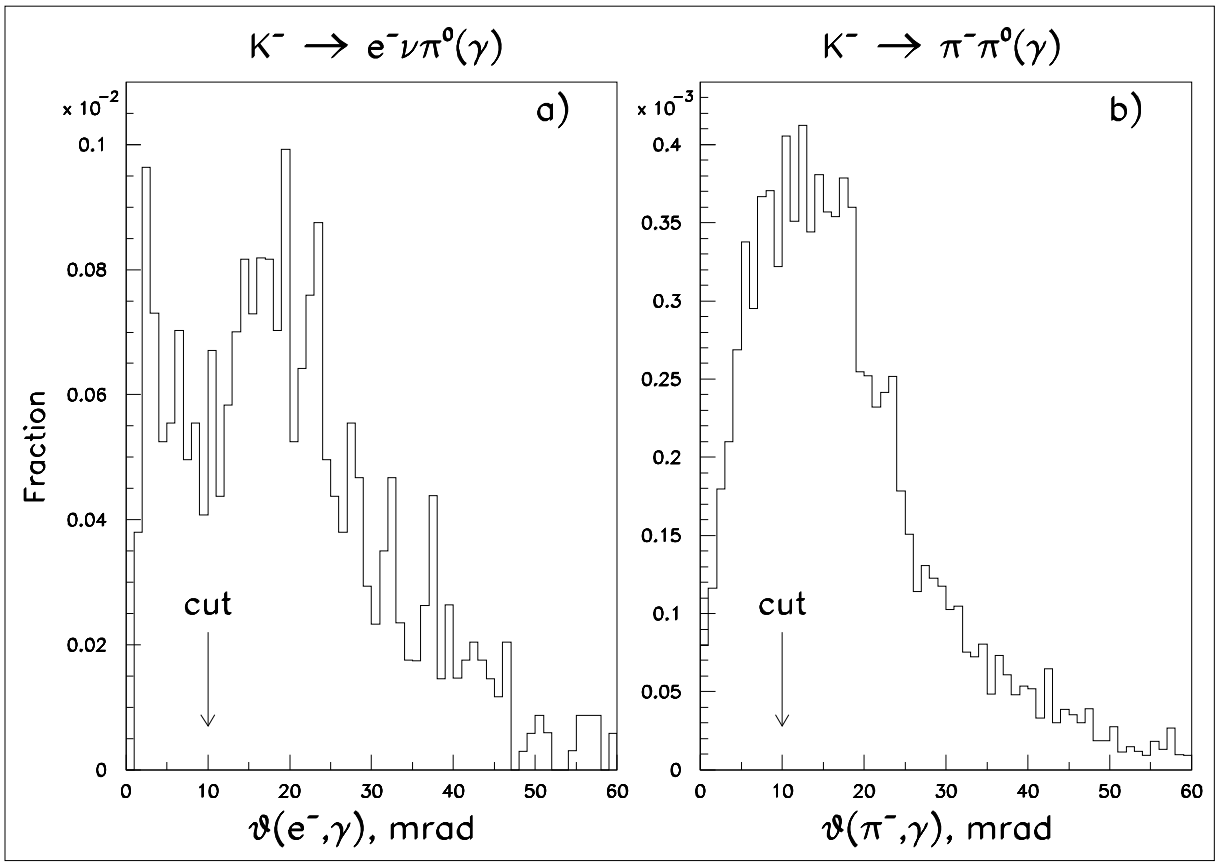

Figure 3: The distributions of the angle in the laboratory system between the secondary track direction and the prompt photon in the $K^- \to e^- \bar{\nu}_e \pi^0(\gamma)$ events (**a**) and in the $K^- \to \pi^- \pi^0(\gamma)$ events (**b**).

At *the third step* of the event selection the hits found in the hodoscope MH, in the proportional chamber PC1 and in the drift tubes DT are considered to minimize the background contamination and systematics. The further selection is done by the requirements:

- the number of hits, which are found in the chamber PC1, but not used in the track reconstruction, is no more than one for each coordinate plane ($\mathcal{P} = 0.85$);
- exactly one hit is detected in the hodoscope MH, and this hit is associated with the secondary track extrapolation to the hodoscope ($\mathcal{P} = 0.80$);
- any hit found in the DT x- or y-coordinate plane is either used in the track reconstruction or associated (in terms of the distance in the DT coordinate plane, $\delta x < 1$ cm or $\delta y < 1$ cm) with at least one SP1 photon interpolation to the drift tubes ($\mathcal{P} = 0.87$).

Depending on the method used in this study, one of the following sets of requirements is added to the selection criteria listed above. There are three sets of such additional requirements: *1)* the strong requirements for the $K^- \to e^-\bar{\nu}_e\pi^0$ selection, *2)* the strong requirements for the $K^- \to \pi^-\pi^0$ selection and *3)* the weak requirements for the $K^- \to \pi^-\pi^0$ selection.

The additional *strong* selection of the $K^- \to e^-\bar{\nu}_e\pi^0$ events is done by *the first set* of requirements:

- the longitudinal position of the decay vertex is in the region of 7 m $< z <$ 11 m ($\mathcal{P} = 0.76$ with respect to the region of 5 m $< z <$ 11 m);
- the electron energy in the K^- rest frame is less than 0.15 GeV ($\mathcal{P} = 0.22$);
- the number of SP1 showers, which are associated with the secondary track, is equal to one ($\mathcal{P} = 0.43$);
- the secondary track is identified as an electron, i.e. the ratio E_{sh}/p_{tr}, calculated for the shower associated with this secondary track, is in the region of $0.8 < E_{sh}/p_{tr} < 1.2$, where E_{sh} is the shower energy and p_{tr} is the secondary track momentum ($\mathcal{P} = 0.75$);
- the angle in the K^- rest frame between the π^0 and the secondary track (with π^- mass assumption) is in the region of $\cos\theta^*(\pi^0, \pi^-) > -0.85$ ($\mathcal{P} = 0.72$).

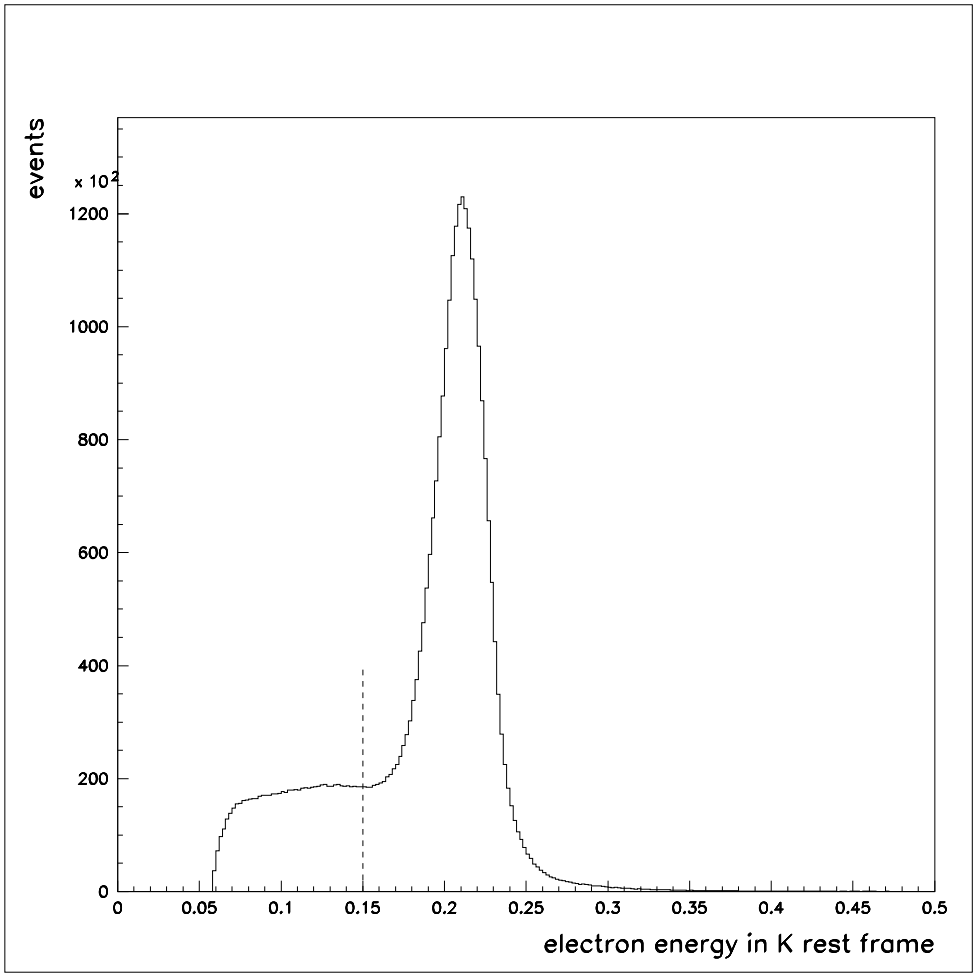
events
x 10^2
1200
1000
800
600
400
200
0
0
0.05
0.1
0.15
0.2
0.25
0.3
0.35
0.4
0.45
0.5
electron energy in K rest frame

The additional *strong* selection of the $K^- \to \pi^-\pi^0$ events is done by *the second set* of requirements:

- the total number of photons is equal to two;
- the longitudinal position of the decay vertex is in the region of 7 m $< z <$ 11 m ($\mathcal{P} = 0.76$ with respect to the region of 5 m $< z <$ 11 m);
- the secondary track is not identified as an electron, i.e. there are no SP1 showers which are associated with the secondary track ($\mathcal{P} = 0.55$);
- the angle in the K^- rest frame between the π^0 and the secondary track (with π^- mass assumption) is in the region of $\cos\theta^*(\pi^0, \pi^-) < -0.9$ ($\mathcal{P} = 0.91$).

The additional *weak* selection of the $K^- \to \pi^-\pi^0$ events is done by *the third set* of requirements:

- the number of SP1 showers, which are associated with the secondary track, is equal to one ($\mathcal{P} = 0.43$).

4 Analysis

4.1 The first method

The mass deviation $M(e^-\bar{\nu}_e\pi^0) - M_{K^-}$ in the selected $K^- \to e^-\bar{\nu}_e\pi^0$ events, where M_{K^-} is the K^- mass and $M(e^-\bar{\nu}_e\pi^0)$ is the effective mass of the $e^-\bar{\nu}_e\pi^0$ system calculated with assumptions that the secondary track is an electron and the $\bar{\nu}_e$ momentum in the K^- rest frame is equal to

$$\vec{p}^{\,*}_{\bar{\nu}_e} \;=\; -(\vec{p}^{\,*}_{e^-} + \vec{p}^{\,*}_{\pi^0}),$$

is shown in Fig. 4a. To select events used in this figure the general selection criteria with the additional strong requirements are applied. After this selection we have collected $N_1 = 30749$ events of the $K^- \to e^-\bar{\nu}_e\pi^0$ decay. It was estimated from the Monte Carlo simulation that the contaminations in such events arising from the background $K^- \to \pi^-\pi^0$ decay and from others decays are equal to 0.24% and 0.75% respectively.

The mass deviation $M(\pi^-\pi^0) - M_{K^-}$ in the selected $K^- \to \pi^-\pi^0$ events, where $M(\pi^-\pi^0)$ is the effective mass of the $\pi^-\pi^0$ system calculated with an assumption that the secondary track is a pion, is shown in Fig. 4b. To select events used in this figure the general selection criteria with the additional strong requirements are applied. But in this (in the first) method of the analysis, in order to reduce background contaminations, the selected events are used if the effective mass of the $\pi^-\pi^0$ system is in the range of $M(\pi^-\pi^0) - M_{K^-} > -0.09$ GeV. The total number of $K^- \to \pi^-\pi^0$ events, selected after all cuts, is $N_2 = 425560$. It was estimated from the Monte Carlo simulation that the contaminations in such events arising from the background $K^- \to e^-\bar{\nu}_e\pi^0$ decay and from others decays are equal to 0.0057% and 0.87% respectively.

The quality of all steps of the selection criteria, which were applied with the additional strong requirements, is illustrated for the selected $K^- \to e^-\bar{\nu}_e\pi^0$ and $K^- \to \pi^-\pi^0$ events by the following distributions. So, the deviation of the $\gamma\gamma$ effective mass from the π^0 mass is shown in Fig. 2, and the distribution of the angle in the laboratory system between the secondary track direction and the prompt photon is shown in Fig. 3.

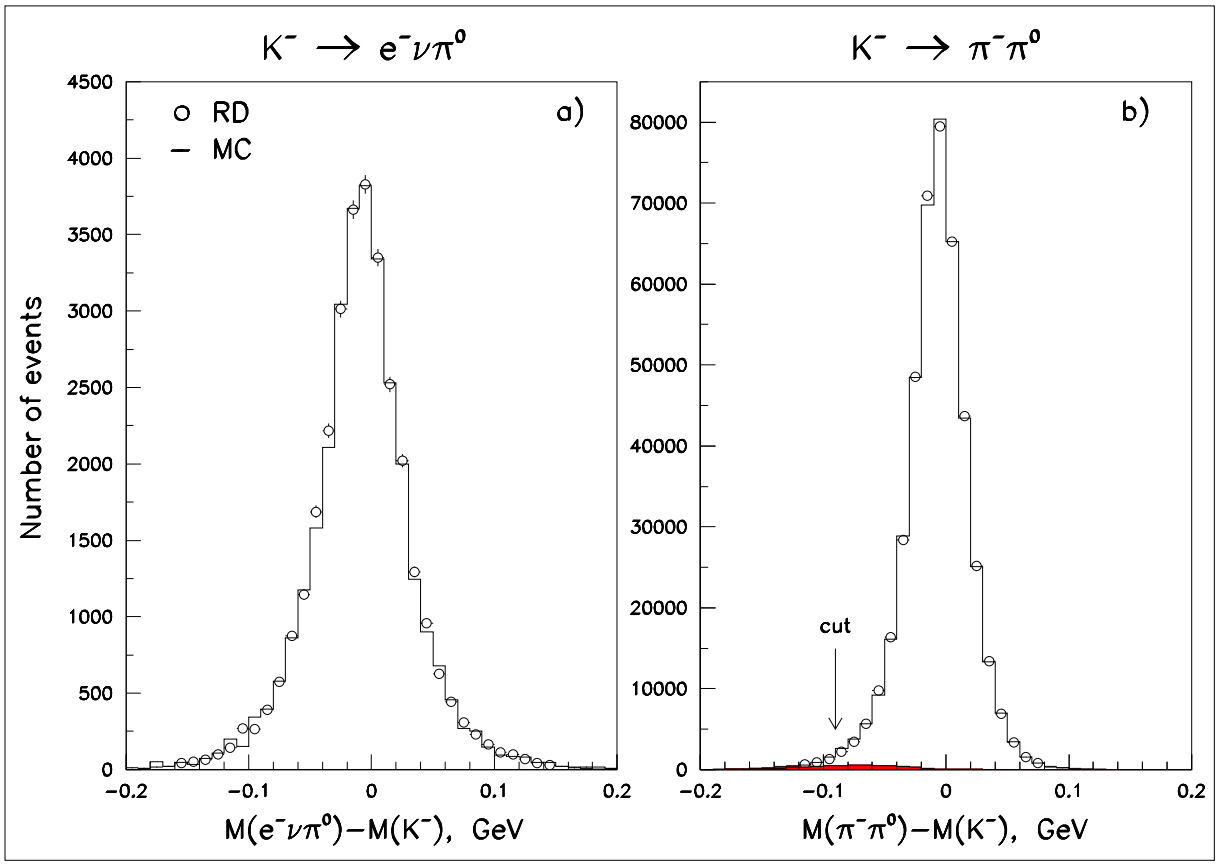

Figure 4: The deviations of the $e^-\bar{\nu}_e\pi^0$ (**a**) and the $\pi^-\pi^0$ (**b**) effective masses from the K^- mass after the third step of the event selection and after the additional strong requirements. The real data (RD) is compared with Monte Carlo simulation (MC). The hatched histogram shows the Monte Carlo estimation of the background contamination.

The ratio $\mathcal{R}_{K_{e3}/K_{2\pi}}$ of branching fractions of the $K^- \to e^-\bar{\nu}_e\pi^0$ and $K^- \to \pi^-\pi^0$ decays can be obtained from the numbers of the selected events (N_1 and N_2) and from the corresponding passing ratios of such events through the experimental setup (P_1 and P_2), estimated from the Monte Carlo simulation. The following value for $\mathcal{R}_{K_{e3}/K_{2\pi}}$ was obtained:

$$\mathcal{R}_{K_{e3}/K_{2\pi}} \equiv \frac{Br(K^- \to e^-\bar{\nu}_e\pi^0)}{Br(K^- \to \pi^-\pi^0)} = \frac{N_1/P_1}{N_2/P_2} = 0.241 \pm 0.0014, \quad (8)$$

where the error is statistical only.

4.2 The second method

The mass deviation $M(\pi^-\pi^0) - M_{K^-}$ in the selected $K^- \to \pi^-\pi^0$ events, where $M(\pi^-\pi^0)$ is the effective mass of the $\pi^-\pi^0$ system calculated with an assumption that the secondary track is a pion, is shown in Fig. 5. To select events used in this figure the general selection criteria and the additional weak requirements are applied. Using these criteria for the $K^- \to \pi^-\pi^0$ decay we have collected $N = 431968$ events. It was estimated from the Monte Carlo simulation that the fractions of the $K^- \to \pi^-\pi^0$, $K^- \to e^-\bar{\nu}_e\pi^0$ and others decays in this sample are equal to 75.9%, 22.5% and 1.6% respectively.

The upper histogram in Fig. 5 is the result of the fit to the real data of the following formula:

$$F(m) = \alpha \cdot [f_1(m) + \frac{r}{R} \cdot f_2(m) + f_3(m)], \tag{9}$$

where $m = M(\pi^-\pi^0) - M_{K^-}$; the fitted value of α provides the normalization; the $f_1(m)$, $f_2(m)$ and $f_3(m)$ terms are the contributions of the $K^- \to \pi^-\pi^0$, $K^- \to e^-\bar{\nu}_e\pi^0$ and others decays; r is the fitted value of the ratio $\mathcal{R}_{K_{e3}/K_{2\pi}}$; R is the fixed value of the same ratio which is used in the Monte Carlo simulation. The $f_1(m)$, $f_2(m)$ and $f_3(m)$ terms were estimated from the events simulated by Monte Carlo and passed through the experimental setup. In this fit the following result was obtained:

$$\mathcal{R}_{K_{e3}/K_{2\pi}} \equiv \frac{Br(K^- \to e^-\bar{\nu}_e\pi^0)}{Br(K^- \to \pi^-\pi^0)} = r = 0.244 \pm 0.0015. \tag{10}$$

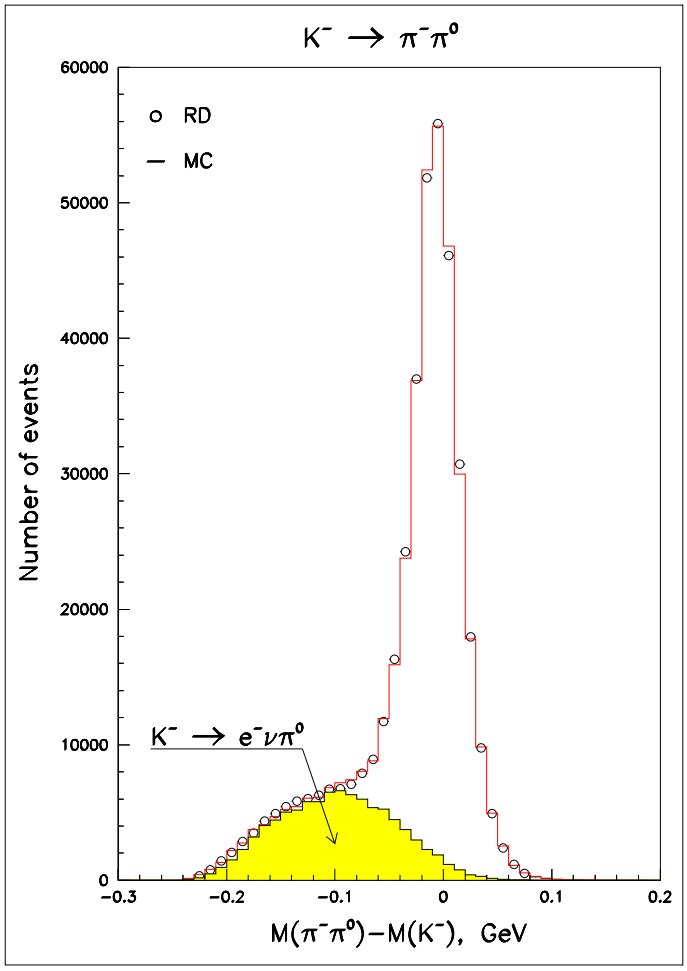

Figure 5: The deviation of the $\pi^-\pi^0$ effective mass from the K^- mass in the $K^- \to \pi^-\pi^0$ events after the third step of the event selection and after the additional weak requirements. The real data (RD) is compared with Monte Carlo simulation (MC). The hatched histogram shows the contribution of the $K^- \to e^-\bar{\nu}_e\pi^0$ decay estimated from the Monte Carlo simulation.

4.3 The third method

Fig. 6 shows the $\cos\theta(\pi^-,\pi^0)$ distribution in $K^- \to \pi^-\pi^0$ events, where $\theta(\pi^-,\pi^0)$ is the angle in the K^- rest frame between the π^0 and π^- mesons calculated with an assumption that the secondary track is a pion. The events used in this figure were selected by the general selection criteria with the additional weak requirements. Applying these criteria for the $K^- \to \pi^-\pi^0$ decay we have collected $N = 431968$ events. It was estimated from the Monte Carlo simulation that the fractions of the $K^- \to \pi^-\pi^0$, $K^- \to e^-\bar{\nu}_e\pi^0$ and others decays in this sample are equal to 75.9%, 22.5% and 1.6% respectively.

The upper histogram in Fig. 6 is the result of the fit to the real data of the following formula:

$$F(m) = \alpha \cdot [f_1(m) + \frac{r}{R} \cdot f_2(m) + f_3(m)], \tag{11}$$

where $m = M(\pi^-\pi^0) - M_{K^-}$; the fitted value of α provides the normalization; the $f_1(m)$, $f_2(m)$ and $f_3(m)$ terms are the contributions of the $K^- \to \pi^-\pi^0$, $K^- \to e^-\bar{\nu}_e\pi^0$ and others decays; r is the fitted value of the ratio $\mathcal{R}_{K_{e3}/K_{2\pi}}$; R is the fixed value of the same ratio which is used in the Monte Carlo simulation. The $f_1(m)$, $f_2(m)$ and $f_3(m)$ terms were estimated from the events simulated by Monte Carlo and passed through the experimental setup. In this fit the following result was obtained:

$$\mathcal{R}_{K_{e3}/K_{2\pi}} \equiv \frac{Br(K^- \to e^-\bar{\nu}_e\pi^0)}{Br(K^- \to \pi^-\pi^0)} = r = 0.242 \pm 0.0015. \tag{12}$$

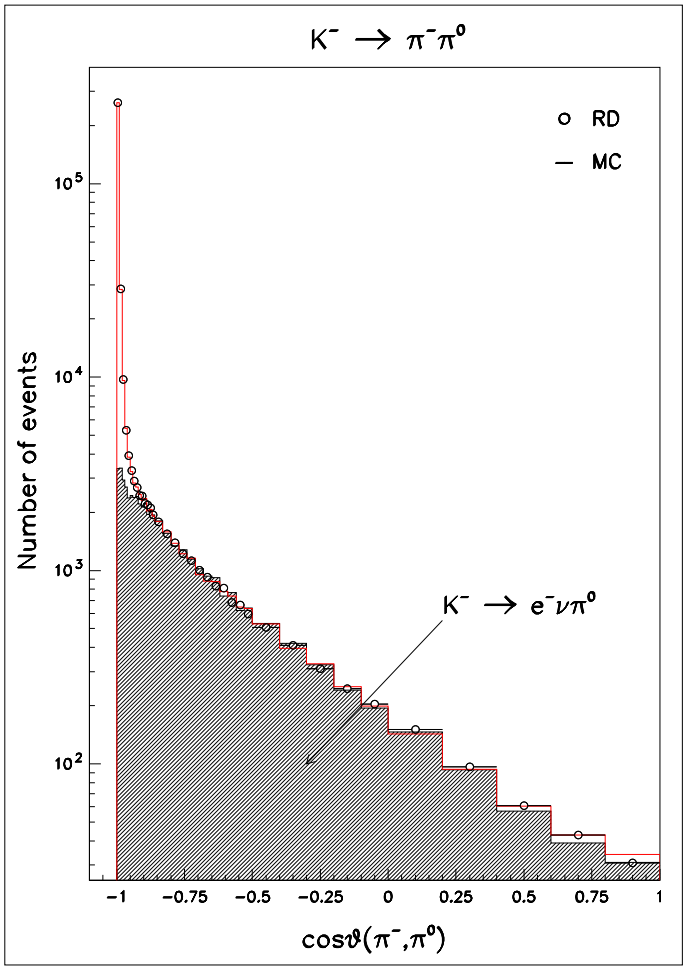

Figure 6: The distribution of cosine of the angle in the K^- rest frame between the π^0 and π^- mesons in the $K^- \to \pi^-\pi^0$ decay after the third step of the event selection and after the additional weak requirements. The real data (RD) is compared with Monte Carlo simulation (MC). The hatched histogram shows the contribution of the $K^- \to e^-\bar{\nu}_e\pi^0$ decay estimated from the Monte Carlo simulation.

4.4 The sources of systematics

In the determination of the systematic uncertainty of $\mathcal{R}_{K_{e3}/K_{2\pi}}$ the following sources of systematics were investigated.

- The matrix elements of the decay modes used in the Monte Carlo simulation were varied within their errors ($\Delta\mathcal{R} = 0.0002$).
- The variations of the background components in the Monte Carlo simulation were allowed ($\Delta\mathcal{R} = 0.0017$).
- The low and upper edges for the decay vertex position were varied along the setup axis ($\Delta\mathcal{R} = 0.0006$).
- The electromagnetic showers, detected in the calorimeter SP2, were not used in the photon reconstruction ($\Delta\mathcal{R} = 0.0002$).
- The energy threshold in the photon selection was varied from the value of 0.8 GeV to 2 GeV ($\Delta\mathcal{R} = 0.0009$).
- The variation of the mass deviation cut for the $\gamma\gamma$ system was applied ($\Delta\mathcal{R} = 0.0004$).
- The variation of the low edge for the relative transverse position between the SP1 photon and the secondary track extrapolation was applied ($\Delta\mathcal{R} = 0.0006$).
- The variation of the upper edge for the relative transverse position between the associated SP1 shower and the secondary track extrapolation was applied ($\Delta\mathcal{R} = 0.0005$).
- The variation of the cut for the probability of the decay vertex fit was applied ($\Delta\mathcal{R} = 0.0006$).

– The variation of the cut for the angle between the K^- line of flight and the secondary track direction in the K^- rest frame (with π^- mass assumption) was applied ($\Delta\mathcal{R}$ = 0.0012).

– The cut for the variable $\xi = E_{sh}/p_{tr}$, which is used in the particle identification, was varied ($\Delta\mathcal{R} = 0.0005$).

– The variation of the mass deviation cut for the $\pi^-\pi^0$ system was applied ($\Delta\mathcal{R}$ = 0.0014).

– The variation of the cut for the angle between the π^- and π^0 directions in the K^- rest frame (with π^- mass assumption) was applied ($\Delta\mathcal{R} = 0.0015$).

– The cut for the angle in the laboratory system between the prompt photon and the secondary track was varied ($\Delta\mathcal{R} = 0.0016$).

– The low edge of the total energy, detected in the SP1, was varied from the threshold to the value of 8 GeV ($\Delta\mathcal{R} = 0.0005$).

5 Result

5.1 $\mathcal{R}_{K_{e3}/K_{2\pi}}$ ratio and K_{e3} branching fraction

The average value obtained from the three methods of this study is the following:

$$\mathcal{R}_{K_{e3}/K_{2\pi}} \equiv \frac{Br(K^- \to e^- \bar{\nu}_e \pi^0)}{Br(K^- \to \pi^- \pi^0)} = 0.2423 \pm 0.0015\,(stat) \pm 0.0037\,(syst), \quad (13)$$

where the first error *(stat)* is statistical and the second one *(syst)* is systematic. Our result can be compared to the current PDG average value of $\mathcal{R}_{K_{e3}/K_{2\pi}} = 0.2455 \pm 0.0023$ [4]. Using the PDG average value for the $K_{2\pi}$ branching fraction, $Br(K_{2\pi}) = 0.2066 \pm 0.0008$ [4], the K_{e3} branching fraction is found to be

$$Br(K_{e3}) = \mathcal{R}_{K_{e3}/K_{2\pi}} \times Br(K_{2\pi}) = \\ = 0.0501 \pm 0.0003\,(stat) \pm 0.0008\,(syst) \pm 0.0002\,(norm), \quad (14)$$

where the third error *(norm)* is the uncertainty of the $K_{2\pi}$ normalisation branching fraction. This final result can be compared to the corresponding PDG average value of $Br(K_{e3}) = 0.0507 \pm 0.0004$ [4].

Table 1: The input values to Eq. (3) and the result for the $|V_{us}|\, f_+(0)$ term.

terms		values	Refs.
Branching fraction,	$Br(K_{e3})$	0.0501±0.0009	this study
Phase space integral,	I_K^e	0.1591±0.0012	[3]
Radiative correction,	$\delta^e_{SU(2)}$	0.0231±0.0022	[2]
Radiative correction,	δ^e_{EM}	0.0003±0.0010	[2]
$\|V_{us}\|\, f_+(0)$		0.2115±0.0021	

5.2 V_{us} matrix element

The $|V_{us}|$ element in the CKM quark mixing matrix can be calculated from the decay rate for the $K^- \to e^-\bar{\nu}_e\pi^0$ decay, combined with theoretical corrections and other experimental measurements (see Eq. (3)).

Using the K_{e3} decay rate measured in this study, the $K^\pm$ lifetime $\tau_{K^\pm} = (1.2380 \pm 0.0021) \times 10^{-8}$ s [4], the Fermi constant $G_{\rm F} = (1.16637 \pm 0.00001) \times 10^{-5}$ GeV^{-2} [11], the $K^\pm$ mass $m_K = 0.493677 \pm 0.000016$ GeV/c^2 [4], $S_{EW} = 1.0230 \pm 0.0003$ [12], the phase space integral I_K^e and long-distance corrections $\delta^e_{SU(2)}$ and δ^e_{EM} as given in Table 1, the $|V_{us}|$ matrix element times the vector form factor $f_+(0)$ is found to be

$$|V_{us}|\, f_+(0) \;=\; 0.2115 \pm 0.0006\,(stat) \pm 0.0017\,(syst) \pm 0.0004\,(norm) \pm 0.0009\,(ext), \quad (15)$$

where the external (ext) error is due to the model-dependent long-distance correction (4) and to the phase space integral (5) evaluated from the quadratic approximations (6)–(7). The form factor value $f_+(0) = 0.9644 \pm 0.0049$ [13] from a three-flavor unquenched lattice QCD calculation gives the following value for the matrix element $|V_{us}|$:

$$|V_{us}| \;=\; 0.2193 \pm 0.0021\,(other) \pm 0.0011\,(theo), \quad (16)$$

where "theo" refers to the theoretical uncertainty due to $f_+(0)$, and "other" refers to all the uncertainties already included in (15).

These values, (15) and (16), are to be compared to the average of the following five decay modes: $K^\pm \to \pi^0 e^\pm \nu$, $K^\pm \to \pi^0 \mu^\pm \nu$, $K^0_L \to \pi e \nu$, $K^0_L \to \pi \mu \nu$ and $K^0_S \to \pi e \nu$. The average of these modes, measured in other experiments, yields $|V_{us}|\, f_+(0) = 0.2166 \pm 0.0005$ and $|V_{us}| = 0.2246 \pm 0.0012$ [4].

6 Conclusion

The ratio of the decay rates for the $K^- \to e^- \bar{\nu}_e \pi^0$ and $K^- \to \pi^- \pi^0$ decays has been measured using the ISTRA+ spectrometer. The result of our measurement is the following:

$$\mathcal{R}_{K_{e3}/K_{2\pi}} = 0.2423 \pm 0.0015\,(stat) \pm 0.0037\,(syst). \tag{17}$$

Using the current experimental knowledge of the $K^- \to \pi^- \pi^0$ branching fraction, this result leads to the measured branching fraction of $Br(K_{e3}) = 0.0501 \pm 0.0009$ and to the value of $|V_{us}|\, f_+(0) = 0.2115 \pm 0.0021$.

The work is supported by the Russian Fund for Basic Research (grant No. 11-02-00870-a).

References

[1] H. Leutwyler, M. Roos, *Z. Phys.*, **C25** (1984) 91.

[2] V. Cirigliano et al., *Eur. Phys. J.*, **C35** (2004) 53;
V. Cirigliano et al., *Eur. Phys. J.*, **C23** (2002) 121;
E.S. Ginsberg, *Phys. Rev.*, **D1** (1970) 229;
E.S. Ginsberg, *Phys. Rev.*, **162** (1967) 1570;
E.S. Ginsberg, *Phys. Rev.*, **187** (1969) 2280;
E. Blucher et al., Proceedings of the CKM 2005 Workshop (WG1), UC San Diego, 15-18 March 2005.

[3] J.R. Batley et al., *Eur. Phys. J.*, **C50** (2007) 329.

[4] *Particle Data Group*, J. Beringer et al., *Phys. Rev.*, **D86** (2012) 010001.

[5] V.I. Romanovsky et al., Preprint IHEP 2007-5, Protvino, 2007.

[6] V.N. Bolotov et al., Preprint IHEP 95-111, Protvino, 1995.

[7] I.V. Ajinenko et al., *Yad. Fiz.*, **65** (2002) 2125;
I.V. Ajinenko et al., *Phys. At. Nucl.*, **65** (2002) 2064;
I.V. Ajinenko et al., *Phys. Lett.*, **B574** (2003) 14;
O.P. Yushchenko et al., *Phys. Lett.*, **B589** (2004) 111.

[8] I.V. Ajinenko et al., *Yad. Fiz.*, **66** (2003) 107;
I.V. Ajinenko et al., *Phys. At. Nucl.*, **66** (2003) 105;
O.P. Yushchenko et al., *Phys. Lett.*, **B581** (2004) 31.

[9] I.V. Ajinenko et al., *Phys. Lett.*, **B567** (2003) 159.

[10] R. Brun et al., Preprint CERN-DD/EE/84-1.

[11] A. Czarnecki, W.J. Marciano, A. Sirlin, *Phys. Rev.*, **D70** (2004) 093006.

[12] A. Sirlin, *Nucl. Phys.*, **B196** (1982) 83.

[13] P.A. Boyle et al., *Phys. Rev. Lett.*, **100** (2008) 141601.